

PAPER

CrossMark
click for updatesCite this: *RSC Adv.*, 2015, 5, 29799

Plasma-based dry reforming: improving the conversion and energy efficiency in a dielectric barrier discharge†

R. Snoeckx,^{*a} Y. X. Zeng,^b X. Tu^{*b} and A. Bogaerts^a

Dry reforming of methane has gained significant interest over the years. A novel reforming technique with great potential is plasma technology. One of its drawbacks, however, is energy consumption. Therefore, we performed an extensive computational study, supported by experiments, aiming to identify the influence of the operating parameters (gas mixture, power, residence time and “frequency”) of a dielectric barrier discharge plasma on the conversion and energy efficiency, and to investigate which of these parameters lead to the most promising results and whether these are eventually sufficient for industrial implementation. The best results, in terms of both energy efficiency and conversion, are obtained at a specific energy input (SEI) of 100 J cm^{-3} , a 10–90 CH_4 – CO_2 ratio, 10 Hz, a residence time of 1 ms, resulting in a total conversion of 84% and an energy efficiency of 8.5%. In general, increasing the CO_2 content in the gas mixture leads to a higher conversion and energy efficiency. The SEI couples the effect of the power and residence time, and increasing the SEI always results in a higher conversion, but somewhat lower energy efficiencies. The effect of the frequency is more complicated: we observed that the product of frequency (f) and residence time (τ), being a measure for the total number of micro-discharge filaments which the gas molecules experience when passing through the reactor, was critical. For most cases, a higher number of filaments yields higher values for conversion and energy efficiency. To benchmark our model predictions, we also give an overview of measured conversions and energy efficiencies reported in the literature, to indicate the potential for improvement compared to the state-of-the-art. Finally, we identify the limitations as well as the benefits and future possibilities of plasma technology.

Received 19th January 2015

Accepted 18th March 2015

DOI: 10.1039/c5ra01100k

www.rsc.org/advances

Introduction

The conversion of the main greenhouse gases, CO_2 and CH_4 , into value added chemicals and liquid fuels is considered as one of the main challenges for the 21st century.^{1,2} The combined reforming of both CH_4 and CO_2 , *i.e.*, dry reforming of methane (DRM), has therefore gained significant interest over the years because of its (possible) environmental impact.^{3,4} Its main advantages over other reforming processes are the use of CO_2 as both a carbon source and oxidizing agent and the production of syngas (H_2/CO) in a ratio which is easily controllable. The main disadvantage for implementing catalytic DRM on an industrial scale is its inherent carbon deposition, which leads to catalyst poisoning.⁵ Nevertheless, as stated by Mikkelsen *et al.*⁶ ‘The

formation of synthesis gas by dry reforming of methane could provide a substantial use for CO_2 from industrial and natural sources. This capture provides a renewable, inexhaustible carbon source and could also provide a means for the continued use of derived carbon fuels in an environmental friendly and carbon neutral way.’ As a result, the interest for alternative (non-conventional) reforming technologies grew quickly and one of the alternatives which is considered to have great potential in this area is plasma technology.⁷

The advantage of non-thermal plasmas, compared to the classical catalytic process, is that the gas can remain near room temperature while being “activated” by electron impact excitation, ionization and dissociation reactions. Furthermore, higher conversions and selectivities can be obtained without problems of carbon deposition.⁸ The energy required for sustaining a plasma is provided by electricity, which at first seems to limit its use as a greenhouse gas mitigation technology, since in general producing electricity results in CO_2 emissions. The type of plasma which is currently most often used for DRM (and gas conversion in general) is the dielectric barrier discharge (DBD). Tao *et al.*⁸ calculated that for every mole CO_2 reformed in a DBD, one mole CO_2 would be emitted if the electricity came from methane combustion. Furthermore, in

^aResearch Group PLASMANT, Department of Chemistry, University of Antwerp, Antwerp, Belgium. E-mail: ramses.snoeckx@uantwerpen.be; xin.tu@liverpool.ac.uk

^bDepartment of Electrical Engineering and Electronics, University of Liverpool, Liverpool L69 3GJ, UK

† Electronic supplementary information (ESI) available: The ESI contains (a) an overview of the detailed experimental and computational results, used for the model validation; as a function of the CH_4 – CO_2 ratio, the residence time and the SEI. (b) All graphs and a more extensive description of the influence regarding gas ratio in the entire range of conditions. See DOI: 10.1039/c5ra01100k

our previous work⁹ we calculated that the energy efficiency of plasma-based DRM would need to achieve a theoretical energy efficiency of at least ~60% to be competitive with classical DRM.

Nevertheless, plasma technology is attracting a lot of attention because of several advantages over conventional gas conversion techniques. One of those advantages is closely related to the worldwide transition to renewable energy sources, such as solar and wind energy. The large scale adoption of these renewable energy sources poses a challenge for efficient storage and easy transport of the electricity produced (*i.e.*, during peak moments on the grid). While storage in batteries is possible, it is less efficient than chemical storage in fuels.¹⁰ Such fuels, often referred to as carbon neutral fuels or solar fuels, offer a much higher gravimetric and volumetric energy storage capacity, they have much higher energy densities than electrical storage techniques and they match the existing worldwide liquid fuel infrastructure.^{6,10} As such, the current transition to renewable energy sources does not only give plasma processes a clean electricity source, but because of the high operation flexibility, *i.e.*, plasmas can be turned on and off quickly, they are very suitable for storing intermittent sustainable energy in a chemical form. More specifically, the syngas produced in this way can then be chemically processed into chemicals and fuels, for example by using the conventional Fischer-Tropsch process.¹¹

However, plasma technology is not the only player in this field and one of its drawbacks, especially of a DBD, is the energy consumption, which is currently still too high for industrial application, even when using sustainable energy sources.^{8,9} Therefore, in the present paper, we perform an extensive computational optimization study for a DBD, based on a model that we developed and validated before.⁹ Moreover, some new experiments are performed to support the model in this broader parameter range. The aim of this study is to identify the influence of the operating parameters of a DBD for DRM and to investigate which of these parameters are most promising in terms of energy efficiency and conversion and whether this is eventually sufficient for industrial implementation or whether different plasma set-ups (*i.e.*, packed-bed DBD^{7,12} or so-called warm plasmas^{7,8,13-16}) should be pursued.

Description of the model

0D chemical kinetics model

The model used in this work to describe the plasma chemistry is a zero-dimensional (0D) kinetic model, called Global_kin, developed by Kushner and co-workers.¹⁷ This model calculates the time-evolution of the species densities, based on the production and loss terms defined by the chemical reactions. An energy balance equation calculates the electron temperature, which is used by the Boltzmann equation module to calculate the rate coefficients of the electron impact reactions. For a more detailed description of the model, we refer to our previous work.⁹

Plasma chemistry included in the model

The chemistry set used in this model was developed and experimentally validated in our previous work.⁹ It considers 62

different species, which react with each other in 121 electron impact reactions, 87 ion reactions and 290 neutral reactions. Their corresponding rate coefficients and the references where these data were adopted from are listed in the ESI of our previous work.⁹

Description of a filamentary DBD setup in the model

DBDs typically operate in the filamentary regime, consisting of a large number of micro-discharge filaments,¹⁸ which present themselves in the electrical current waveform as many short peaks. Describing these filaments in a plasma model is not straightforward, because of their distribution in time and space. Nonetheless, including a realistic description of these filaments is indispensable to obtain a realistic description of the plasma chemistry. One might argue that a 0D model seems unfit for this task, since it only allows simulating the plasma behavior as a function of time, and not as a function of space. However, this temporal behavior can easily be translated into a spatial behavior, by means of the gas flow, allowing us to mimic the filamentary behavior by simulating a large number of micro-discharge pulses as a function of time. This approach has already proven to be applicable for a variety of conditions and gas mixtures.^{9,19-22} A more detailed description of this method can be found in our previous work.⁹

Calculation of conversion and energy efficiency

To identify the most energy efficient operating conditions, we varied the following parameters in a wide range: gas composition, specific energy input (SEI), gas residence time and “frequency” (see below). The critical calculation output in this assessment will be the total conversion and the energy efficiency of the process.

The conversion of CH₄ and CO₂ is defined as:

$$\chi_i = \frac{\text{moles of } i \text{ converted}}{\text{moles of } i \text{ input}}; \quad (1)$$

where $i = \text{CH}_4$ or CO_2

The total conversion can then be written as:

$$\chi_{\text{Total}} = \text{fraction CO}_2 \cdot \chi_{\text{CO}_2} + \text{fraction CH}_4 \cdot \chi_{\text{CH}_4} \quad (2)$$

Furthermore, the energy efficiency is determined as follows:

$$\eta = \frac{\chi_{\text{Total}} \cdot \Delta H_{298 \text{ K}}^0}{\text{SEI}} = \frac{\chi_{\text{Total}} \cdot 2.56 \text{ (eV per molecule)}}{\text{SEI (eV per molecule)}} \quad (3)$$

where SEI is the specific energy input, defined as (for room temperature and atmospheric pressure):

$$\begin{aligned} \text{SEI (J cm}^{-3}\text{)} &= \text{SEI (eV per molecule)} \cdot 2.446 \times 10^{19} \\ &\quad (\text{molecule cm}^{-3}) \cdot 1.602 \times 10^{-19} \text{ (J eV}^{-1}\text{)} \\ \Leftrightarrow \text{SEI (J cm}^{-3}\text{)} &= \text{SEI (eV per molecule)} \cdot 3.92 \\ \Leftrightarrow \text{SEI (J cm}^{-3}\text{)} &= \frac{\text{Power (W)}}{\text{Flow rate (ml min}^{-1}\text{)}} \cdot \frac{60 \text{ (s min}^{-1}\text{)}}{1 \text{ (cm}^3 \text{ ml}^{-1}\text{)}} \quad (4) \end{aligned}$$

Explanation of the parameters varied in this study

The parameters varied in this study are as follows:

- CH₄-CO₂ gas composition (%): 90–10, 75–25, 50–50, 25–75, 10–90;
- SEI (J cm⁻³): 0.01, 0.1, 1, 10, 100;
- Residence time (s): 0.001, 0.01, 0.1, 1, 10, 100;
- Frequency (kHz): 0.01, 0.1, 1, 10, 100.

Hence, it is clear that for every gas composition 150 different combinations are possible, bringing the total number of numerically investigated cases to 750.

Note that the values of these parameters are chosen based on typical values reported in literature, *i.e.*, a residence time ranging from 1 till 100 s, a SEI going from 1 till 100 J cm⁻³ and a frequency in the order of 1 to 100 kHz are commonly reported.^{8,9,23–28} However, besides these typical values, we also want to explore new regions of these parameters, which are to date not yet reported, *e.g.*, a residence time of 0.001 s, coupled with an SEI of 0.1 J cm⁻³, which might be pursued for micro-reactors.^{29,30} This is exactly the strength of computer simulations to go beyond the classical conditions and to predict whether new conditions could be more promising, and thus whether experimentally the construction of new reactor types or power set-ups should be pursued.

For the interpretation of the calculation results it is important to understand how the variation of these parameters relates to experiments. The gas composition, SEI and residence time can be directly compared to experiments (through the experimental gas flow rate, reactor volume and power). However, the variation of the “frequency” is a more complex story, which can be looked at from two different angles. (a) On one hand, if we assume that the average number of filaments that occur during each half cycle of the applied voltage is constant, varying the frequency is a way to control the total number of filaments that occur during a certain residence time of the gas, and thus the energy deposited in each filament (keeping the total applied power constant). In this case, the “frequency” directly corresponds to the experimental frequency of the applied voltage. (b) Another way to interpret the “frequency” is when the number of filaments that occur during each half cycle is not constant but varies with the operating conditions. Then, a higher (or lower) “frequency” corresponds to a larger (or smaller) number of filaments during each half cycle, with a lower (or higher) energy deposition per filament. To our knowledge, it is not yet known from literature whether (and how) the number of filaments per half cycle changes for a CH₄-CO₂ gas mixture, depending on the operating conditions. It is well possible that for certain conditions or experimental set-ups assumption (a) is valid, while for other conditions, case (b) is valid, or even a combination of both. This meaning of the “frequency” should thus be kept in mind in the following sections, but in any case, the frequency is directly proportional to the total number of filaments for a fixed gas residence time.

Experimental

Plasma reactor

The experiments are carried out in a coaxial DBD reactor. A stainless steel mesh (ground electrode) is wrapped over the

outside of a quartz tube with an outer and inner diameter of 22 and 19 mm, respectively, while a stainless steel rod with an outer diameter of 14 mm is placed in the center of the quartz tube and used as high voltage electrode. The length of the discharge region is 90 mm with a discharge gap of 2.5 mm. CH₄ and CO₂ are used as feed gases with a variable total flow rate of 25–200 ml min⁻¹ and a CO₂-CH₄ molar ratio from 1 : 9 to 9 : 1. The DBD reactor is supplied by a high voltage AC power supply with peak-to-peak voltage of 10 kV and frequency of 50 Hz. The *Q-U* Lissajous method is used to calculate the discharge power.

Product analysis

The feed and product gases are analyzed by a two-channel gas chromatograph (Shimadzu GC-2014) equipped with a flame ionization detector (FID) and a thermal conductivity detector (TCD). The GC is calibrated for a wide range of gases using reference gas mixtures (Air Liquide).

Experimental parameter range

Although our model was validated before,⁹ several additional experiments were performed for this work, to assure that the model, and especially the chemistry set, behave in a realistic manner for conditions beyond the previously validated range.⁹ However, as the total parameter range under investigation is quite large, still only a small part of it could be probed experimentally. This is exactly the aim of our simulations, *i.e.*, by identifying the effects of the above mentioned parameters and subsequently searching for the optimal conditions, we can save a lot of work on expensive and time consuming experiments.

The experimental parameters selected for this additional model validation are listed in Table 1 for a fixed applied frequency of 50 Hz. This parameter selection is limited, because it is based on one experimental setup, *i.e.*, reactor (volume), power supply, mass flow controllers, and this of course restricts the experimental range that is possible. The range could have been made wider if experiments would have been performed with different set-ups, but this would have introduced more unknown variables and effects, which we want to avoid. To allow a one-to-one comparison between model and experiments, we performed additional simulations besides the parameter range already mentioned, to mimic the exact experimental conditions.

Results and discussion

First, we will show the comparison between the model and experimental results, explaining the effect of the various parameters on the conversion and energy efficiency. Subsequently, the general influence of these parameters will be discussed in more detail, as observed for the entire simulation range, to reveal the optimum conditions. Finally, we will compare our model predictions with literature and we will identify the limitations as well as the benefits and future possibilities.

In this study, we focus only on the total conversion and resulting energy efficiency, and not on the selectivity of the

Table 1 Experimental parameters selected for the model validation. The applied frequency was equal to the 50 Hz of the power supply

Gas mixture CH ₄ -CO ₂ (%)	Residence time (s)	Power (W)	SEI (J cm ⁻³)
90-10	32.57	15	36
		7.5	18
75-25	32.57	15	36
		7.5	18
50-50	32.57	15	36
		7.5	18
	16.29	15	18
		7.5	9
	10.86	15	12
		7.5	6
8.14	15	9	
	7.5	4.5	
25-75	32.57	15	36
		7.5	18
		7.5	2.25
10-90	32.57	15	36
		7.5	18

formed products. However, in general, the following trends regarding the product distributions were observed. At high CO₂ contents, the main products are the molecules typically formed in CO₂ splitting (*i.e.*, CO and O₂), and also a fair amount of H₂O. The reason of its formation was explained in our previous work.²² Upon increasing the CH₄ content, on the other hand, the concentration of the classical dry reforming products (*i.e.*, H₂, C₂H₂, C₂H₄, C₂H₆, C₃H₆, C₃H₈) starts to increase, at the expense of the CO₂ splitting products. Changing the frequency or residence time only had a small effect on the absolute concentrations of the formed products, but no significant effect on the product distributions.

Comparison between model and experiments

Effect of the gas ratio. The total conversion and energy efficiency are plotted in Fig. 1 as a function of the CO₂ fraction in the mixture, for a SEI of 18 and 36 J cm⁻³, for both the experimental (black symbols) and modeling results (open red symbols). The exact values can be found in Table S1 of the ESI.† The total conversion and energy efficiency increase slightly upon addition of more CO₂ in the mixture, followed by a decrease for the highest values. The total conversion is about a factor two higher at 36 than at 18 J cm⁻³, whereas the energy efficiency is slightly lower. The modeling results only slightly overestimate the total conversion for low CO₂ contents (by 13 and 7% for the SEI of 18 and 36 J cm⁻³) and slightly underestimate the total conversion for high CO₂ contents (by 11 and 22% for the SEI of 18 and 36 J cm⁻³). This deviation can be explained by the fact that our chemistry does not take into account the vibrational levels of CO₂, which are of lower importance for a DBD,^{20,31} and that the chemistry set was primarily validated for a 50-50 mixture.⁹ However, the absolute values of both conversion and energy efficiency, as predicted by

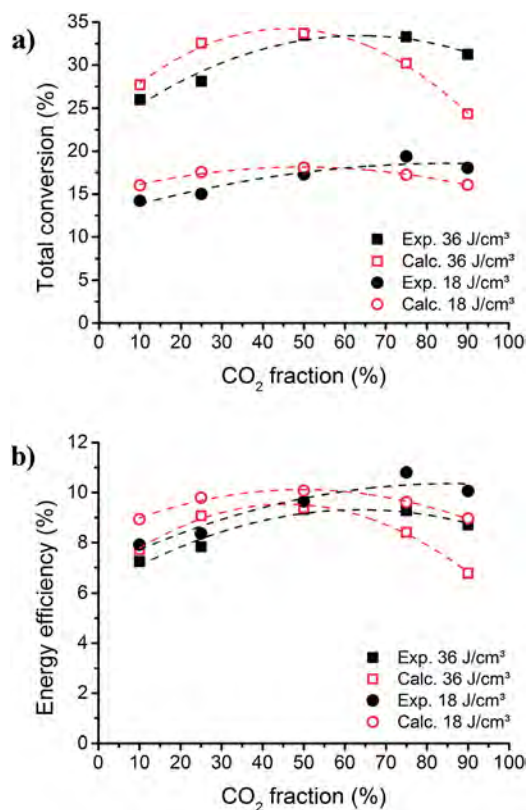


Fig. 1 Calculated and experimental total conversion (a) and energy efficiency (b) as a function of CO₂ fraction, for a SEI of 18 and 36 J cm⁻³.

the model, are generally in good agreement with the experiments, indicating that our model includes the correct plasma chemistry.

Effect of the power, residence time and SEI. In Fig. 2, the total conversion and energy efficiency are plotted as a function of the residence time, for a 50-50 CH₄-CO₂ mixture, at a plasma power of 7.5 and 15 W, for both the experimental (black symbols) and modeling results (open red symbols). The exact values can be found in Table S2 of the ESI.† The experiments were limited to a residence time between 4 and 33 s, but the model was applied to a residence time of 1 and 100 s, for both power values.

It is clear that both in the experiments and the simulations the total conversion is about a factor two higher for a power of 15 W compared to 7.5 W, at the same residence time, which is logical because a higher power yields more (and higher energy) electrons, which can activate the gas and thus initiate the conversion. For the energy efficiency, the trend is less clear. For a residence time ≤ 10 s a higher power yields a slightly higher energy efficiency, whereas for a higher residence time the effect is opposite, but not significant.

Furthermore, when the power is kept constant, the total conversion increases with increasing residence time (which is also straightforward) and the energy efficiency shows the opposite decreasing trend. The latter is most obvious in the calculation results. It follows directly from eqn (3) and (4) above:

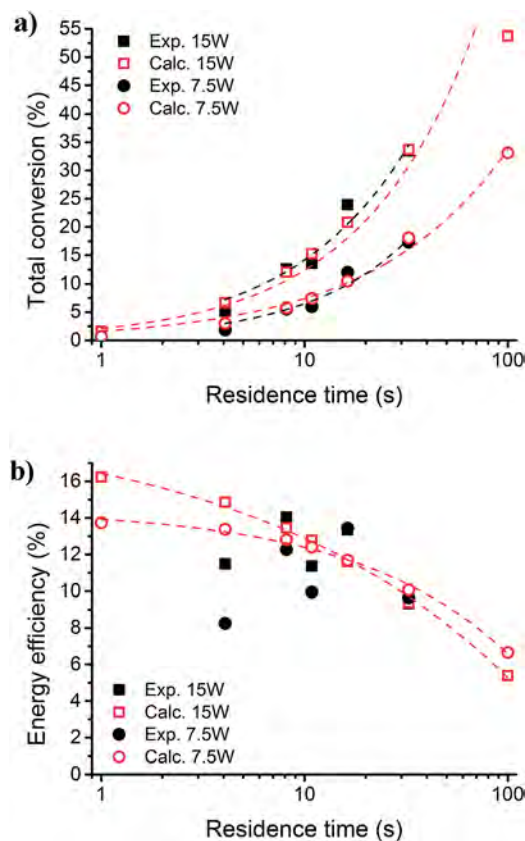


Fig. 2 Calculated and experimental total conversion (a) and energy efficiency (b) as a function of residence time, for a 50–50 CH_4 – CO_2 mixture, and a plasma power of 7.5 and 15 W.

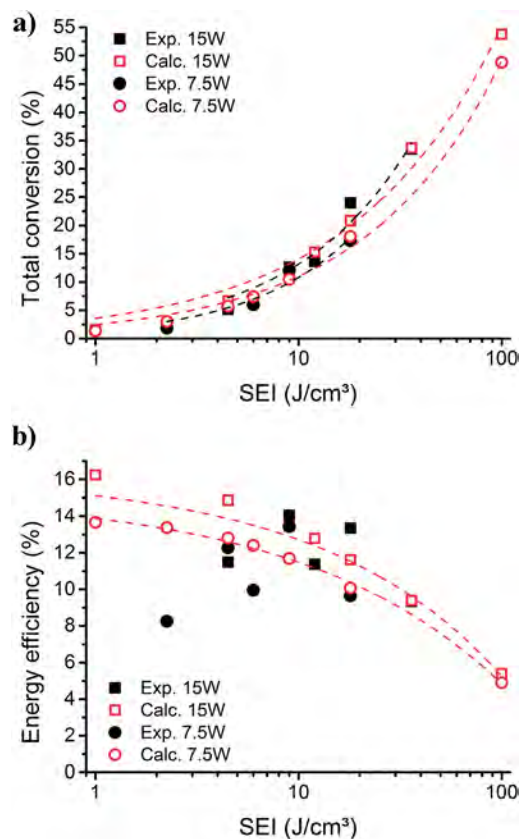


Fig. 3 Calculated and experimental total conversion (a) and energy efficiency (b) as a function of SEI, for a 50–50 CH_4 – CO_2 mixture, and a plasma power of 7.5 and 15 W.

a higher residence time corresponds to a lower flow rate, and thus a higher SEI, at constant power (*cf.* eqn (4)). If the SEI increases more than the conversion, upon increasing residence time, this results in a drop in the energy efficiency (*cf.* eqn (3)).

The effect of the residence time and power can also be combined by plotting the total conversion and energy efficiency as a function of the SEI, as shown in Fig. 3, for a plasma power of 7.5 and 15 W and corresponding residence times as reported in Table 1. Note that the model is again applied in a broader range than could be investigated in the experiments, *i.e.*, four extra points were added for an SEI of 1 and 100 J/cm^3 , for both power values.

It is clear that the SEI is the major determining factor for the conversion and energy efficiency, as it combines the effect of power and residence time (see eqn (4)). Indeed, at the same SEI, increasing the power (thus lowering the residence time) does not affect the total conversion, which remains practically the same at constant SEI. The energy efficiency shows somewhat more variations, when varying the power or residence time, at constant SEI, but these variations are still within a few %.

In general, we may conclude that the calculation and experimental results are again in reasonable agreement, so that we can be confident about the predictive nature of our model, and use it to investigate the effect of the operating conditions in a wider range, beyond what is typically accessible for (standard) experiments.

Model predictions in a wider parameter range

We have systematically studied the effect of all individual parameters, by means of 750 simulations (see above), of which the detailed graphs can be found in the ESI.† In this section, we will show the combined effects, and summarize the general results by means of a few graphs, to elucidate the optimum conditions both in terms of conversion and energy efficiency.

Effect of the gas ratio. Fig. 4 illustrates the calculated energy efficiency plotted as a function of the total conversion, for the best results (solid lines, full symbols) and worst results (dashed lines, open symbols), obtained with the model for all (750) conditions under study. The different gas mixtures are represented by the different colored symbols (see legend) and the different SEI values are also indicated. The conditions at which the maximum and minimum values of conversion and energy efficiency were reached for each CH_4 – CO_2 mixture can be found in Table S3 and S4 of the ESI.†

It is clear that a larger amount of CO_2 leads to a higher total conversion and energy efficiency. This trend is certainly true for the best conditions (solid lines, full symbols). For example, with increasing CO_2 content, the maximum achieved energy efficiency goes from 11.4 to 15.1%. For the worst conditions, the same trend can be observed for the low SEI values, but for the higher SEI values (10 and 100 J/cm^3), the frequency and residence time start to play a role, and depending on the product of

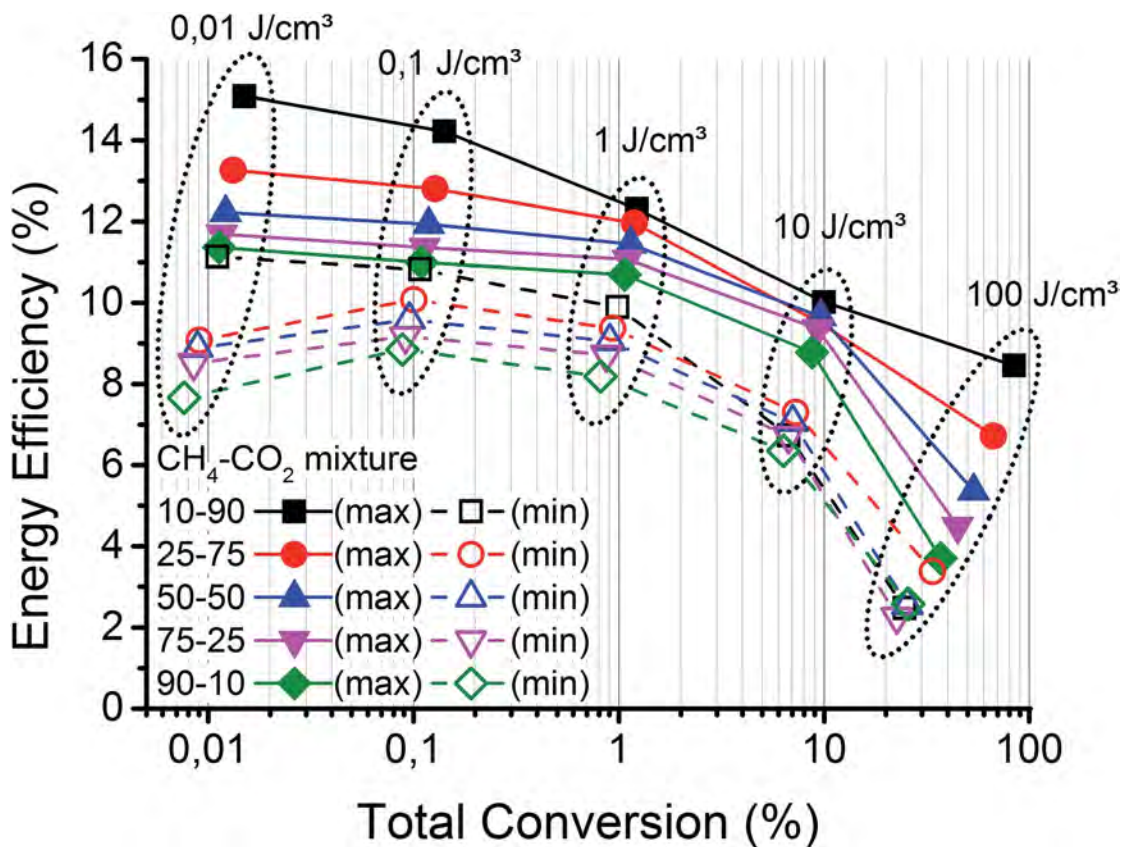


Fig. 4 Maximum and minimum achieved values of energy efficiency vs. total conversion, as obtained from the calculations, for all conditions investigated. The different SEI values are identified with the labels above the curves.

both, a slightly different trend can be observed. These trends are elaborated in detail in the ESI (see Fig. S1–S10).[†] Summarized, in general, the higher total conversion and energy efficiency at larger CO_2 contents is attributed to the O atoms formed by electron impact dissociation of CO_2 , which react very effectively with the H atoms originating from electron impact dissociation of CH_4 . As shown in our kinetic analysis⁹ the conversion of CH_4 is normally limited by the fast backward reaction, $\text{CH}_3 + \text{H} \rightarrow \text{CH}_4$, but when more O atoms are available, this reaction is of minor importance compared to the reaction $\text{O} + \text{H} \rightarrow \text{OH}$. Thus, by limiting the backward reaction, the conversion of CH_4 rises dramatically with increasing CO_2 content, leading to a higher total conversion.

Effect of the power, residence time and SEI. Since the residence time and power are coupled through the SEI (see eqn (4) above), the same trends are observed when increasing either the power or the residence time. Therefore, we will describe their effect simultaneously, by means of the variation in SEI. At all conditions investigated, increasing the SEI at a constant gas ratio and frequency, results in a higher total conversion, as is clear from Fig. 4. This is logical, and was explained above. However, the increase in conversion is not entirely proportional to the rise in SEI, resulting in somewhat lower energy efficiencies with increasing SEI (*cf.* eqn (4)). The highest energy efficiency (*i.e.*, at the lowest SEI of 0.01 J cm^{-3} and a 10–90 $\text{CH}_4\text{--CO}_2$ ratio) is 15.1%, but this corresponds to

very low values for the total conversion (*i.e.*, 0.015%). On the other hand, the highest total conversion (*i.e.*, 84.2%, at the highest SEI value of 100 J cm^{-3} and again a 10–90 $\text{CH}_4\text{--CO}_2$ ratio) corresponds to an energy efficiency of 8.5%. The same trade-off between conversion and energy efficiency has also been reported in previous studies.^{9,23,24} The obtained values will be discussed in more detail, and compared with literature values below.

Effect of the frequency. As described above the interpretation of the frequency is the most difficult to grasp, but it is in any case linked to the number of micro-discharge filaments that occur in the reactor within a certain residence time. At first sight the calculated conversion as a function of frequency did not show a comprehensible trend or coherency. However, it is observed that all of the maximum achieved conversions and energy efficiencies, for all gas mixtures in Fig. 4, are obtained at either a residence time of 100 s and a frequency of 10 kHz, or a residence time of 10 s and a frequency of 100 kHz, except for an SEI of 10 and 100 J cm^{-3} for the 10–90 $\text{CH}_4\text{--CO}_2$ mixture and at 100 J cm^{-3} for the 25–75 mixture, where a residence time of 0.001 s and a frequency of 0.1 kHz gave the best results. Furthermore, all simulations with a frequency of 100 kHz and a residence time of 100 seconds resulted in a steep decrease in total conversion (see Fig. S1–S10 in the ESI[†]). This led us to believe that the critical factors are not the frequency (f) and residence time (τ), but rather the product of both ($\tau \cdot f$), *i.e.*, the

total number of micro-discharge filaments, which the gas molecules experience when passing through the reactor.

Therefore, in Fig. 5 the conversion and energy efficiency are plotted as a function of the total number of micro-discharge filaments experienced by the gas molecules, for a 50–50 gas mixture and for the different values of SEI investigated (see legend). The graphs for the other gas mixtures can be found in the ESI (S11–S15).†

Keeping in mind that for every gas mixture 150 different simulations are performed (see above), this means that Fig. 5 contains 30 data points per SEI value (*i.e.*, per color symbol). As there are only 7 different combinations of the product $\tau \cdot f$, it means that several data points (more or less) coincide with each other. Hence, as anticipated above, all cases with different values of frequency and residence time, but with the same product $\tau \cdot f$, yield almost identical values for conversion and energy efficiency, at a fixed SEI. Thus, it becomes clear that, for a given gas mixture, both the product $\tau \cdot f$ and the SEI are the main underlying factors determining the plasma chemistry and linking the SEI, residence time and frequency all together.

It is clear from Fig. 5 that, at fixed SEI, increasing the number of micro-discharge filaments leads to a slightly higher conversion and energy efficiency, except for the highest number (200 000), where the opposite trend is seen, and for the highest SEI values of 10 and 100 J cm⁻³, where an initial decrease is observed for a low number of filaments. As mentioned above, all gas mixtures show the same general trends, except in the case of

90% CO₂ for the highest SEI values of 10 and 100 J cm⁻³ and for 75% for an SEI of 100 J cm⁻³, where a lower number of filaments leads to a higher total conversion.

Since in the model the energy is divided equally over all micro-discharge filaments, increasing the number of filaments results in a lower energy deposited per filament. It seems that for most cases (except the ones mentioned before) a higher number of filaments, but with lower energy, yields higher values for conversion and energy efficiency, compared to a lower number of filaments, but with more energy deposited per filament. In general, the effect of the total number of filaments seems more important for the energy efficiency than the SEI (except between 10 and 100 J cm⁻³), while the total conversion seems less affected by the number of filaments than by the SEI, which was explained above.

Comparison with literature and critical analysis of the limitations and possibilities of plasma technology

As mentioned above, the highest total conversion (84.2%) is obtained at the highest SEI (100 J cm⁻³), and a CO₂ content of 90%, yielding an energy efficiency of 8.5%. The highest energy efficiency (15.1%), on the other hand, is found for the lowest SEI (0.01 J cm⁻³) and again a CO₂ content of 90%, but this corresponds to a total conversion of only 0.015%. Furthermore, both the total conversion and energy efficiency increase with increasing CO₂ content, while increasing the SEI results in a higher total conversion but a lower energy efficiency, illustrating the trade-off between both. Considering all operating conditions investigated, it is clear that the best overall results (*i.e.*, combination of conversion and energy efficiency) are obtained for the highest SEI and typically for a large total number of filaments, obtained through a residence time of 10–100 s, combined with a frequency of 100–10 kHz, respectively, except for 90 and 75% CO₂, where a lower number of filaments (obtained through a short residence time of 0.001–0.01 s independent of the frequency), or a higher residence time, combined with a low frequency of 0.1 kHz, led to the best results. Table 2 summarizes the best results obtained for the different gas mixtures.

To compare our results with the current state-of-the-art from literature, Fig. 6 illustrates the various experimental data for energy efficiency *vs.* total conversion, obtained from literature,^{25–28,32,33} in comparison with our simulation results, for all conditions investigated. The experimental conditions from literature, and their corresponding results for conversion and energy efficiency, are summarized in Table 3.

It is clear from Fig. 6 and Table 3 that the operating conditions, especially the SEI values, have a large influence on the obtained conversion and energy efficiency. Most experiments are performed for SEI values between 10 and 100 J cm⁻³, and they give rise to conversions and energy efficiencies in the same order as predicted by our simulations. Especially the agreement with experimental results obtained for different CH₄–CO₂ mixtures (denoted by the colored stars) is remarkable. The results of Goujard *et al.*²⁶ and Ozkan *et al.*³³ show exactly the same trend for the effect of gas mixture (*i.e.*, higher conversion and

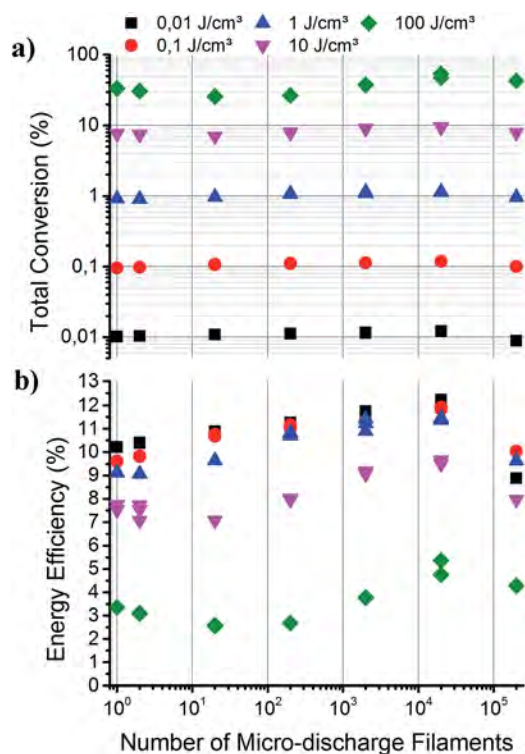


Fig. 5 Calculated conversion (a) and energy efficiency (b) as a function of the total number of micro-discharge filaments for all the different residence times, frequencies and SEI values investigated, for a CH₄–CO₂ mixture of 50–50.

Table 2 Overview of the best results (*i.e.*, combination of conversion and energy efficiency) obtained with the model, for the different gas mixtures

CH ₄ -CO ₂ gas mixture	Conversion	Energy efficiency
90-10	36.9%	3.7%
75-25	44.7%	4.5%
50-50	53.5%	5.4%
25-75	67.0%	6.7%
10-90	84.2%	8.5%

energy efficiency at higher CO₂ content). Furthermore, for a SEI of 100 J cm⁻³ our calculations perfectly match with the results of Zhang *et al.*³² Finally, the results of Wang *et al.*²⁵ indicate a maximum conversion and energy efficiency at 50% CO₂, which can also be explained by our model, because for the high SEI

under consideration, the applied frequency (15.67 kHz) yields good results for low CO₂ content, but at high CO₂ content, lower frequencies would be required.

Besides the good correlation between our model predictions and the literature results, it is also obvious from Fig. 6 that by careful selection of the operating conditions, higher values of energy efficiency (at fixed conversion) or higher conversions (for a given energy efficiency) could be achieved in our model than the values currently reported in literature. Indeed, at a conversion of 10%, the best energy efficiencies found in literature are about 5%, whereas our calculations predict values up to 10%, by careful selection of the frequency, residence time and gas mixture. Furthermore, a conversion of 84.2% with 8.5% energy efficiency, as obtained for 90% CO₂ content (see circle in Fig. 6) is also significantly better than the available experimental data. Also for the other gas mixing ratios, our “best results” (in terms of combination of conversion and

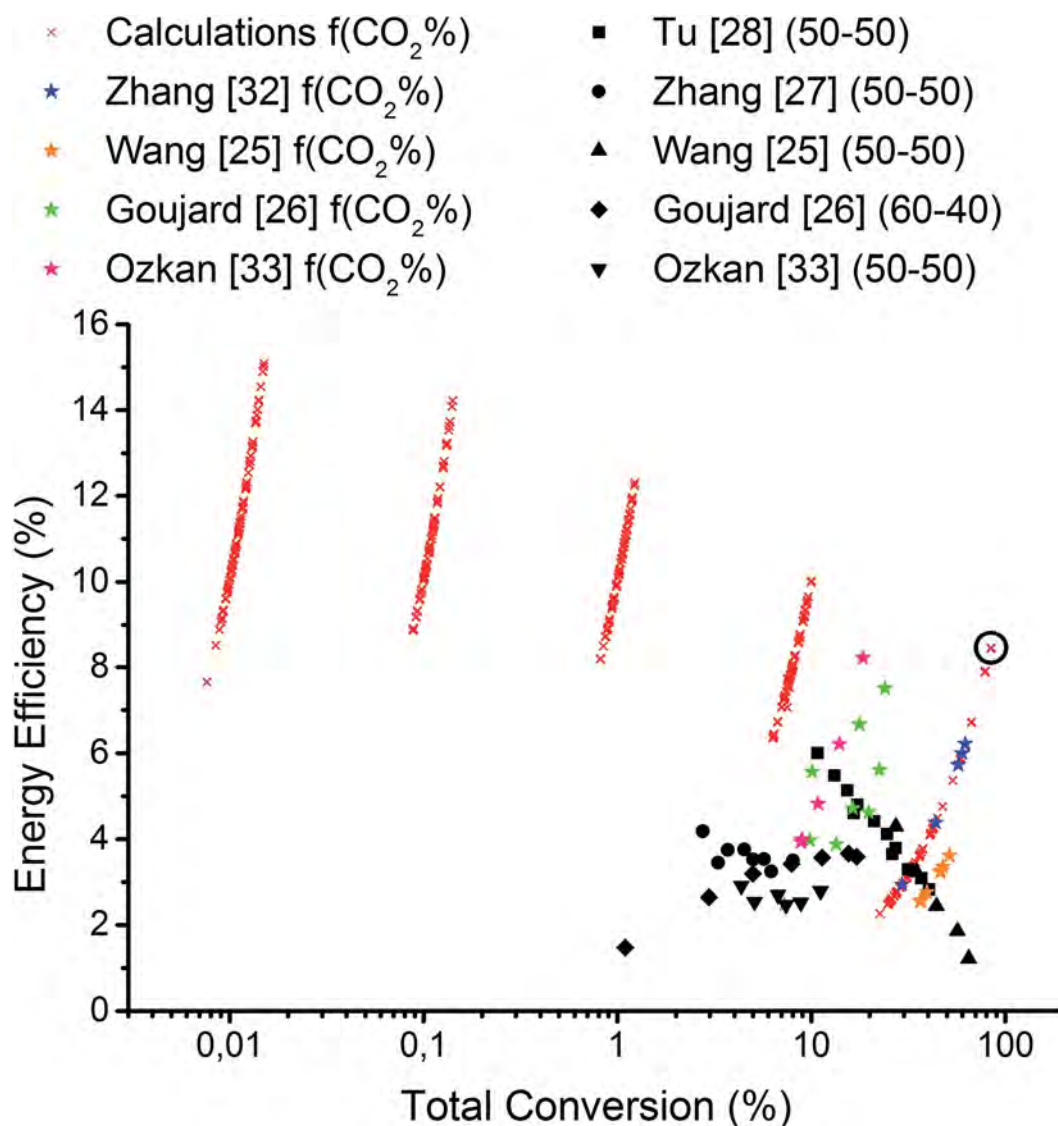


Fig. 6 Comparison between our calculated values of energy efficiency vs. total conversion, for all conditions investigated, with experimental data (obtained for different SEI or as function of CO₂ fraction) collected from literature, as indicated in the legend.

Table 3 Experimental conversions and energy efficiencies collected from literature, for DRM in a DBD, illustrating the current state-of-the-art. When different operating conditions were investigated, the values for the conversion and energy efficiency corresponding to the lower and upper SEI values, are listed. A comparison is also made with values reported for a packed bed DBD, a microwave and a gliding arc plasma (see text)

SEI (J cm^{-3})	Frequency (kHz)	$\text{CH}_4\text{-CO}_2$ (%)	Conversion (%)		Energy efficiency (%)		References
			Lower	Upper	Lower	Upper	
7–23	2.5	50–50	2.8	8.1	4.2	3.5	27
7–48	Pulsed	60–40 ^a	1.1	17.2	1.5	3.6	26
15–40	19.5	50–50 ^b	4.4	11.1	2.9	2.8	33
18–144	30–40	50–50	10.8	40.5	6.0	2.8	28
64–532	15.67	50–50	27.2	64.6	4.3	1.2	25
22.5	19.5	80–20 ^b	8.9	—	4	—	33
		20–80 ^b	—	18.4	—	8.2	
25–40	Pulsed	60–40 ^a	7.26	19.7	2.5	4.6	26
		40–60 ^a	10.1	24	5.6	7.5	
100	25	83–17	—	62	—	6.2	32
		34–66	29.3	—	2.9	—	
143	15.67	83–17	—	46	—	3.2	25
		17–83	36.3	—	2.6	—	
Packed bed DBD							
12	1–100	50–50	27	—	22.6	—	12
Microwave at atm pressure							
18	Pulsed	60–40	70	—	39.0	—	8
Gliding arc							
11.4	10–20	50–50	35.5	—	31.2	—	13
Gliding arc							
1.32–3.96	0.05	50–50	9.8	13.9	74.6	35.2	14

^a Experiments diluted in N_2 . ^b Experiments diluted in Ar.

energy efficiency; *cf.* Table 2) are better than the results reported to date in literature (see Table 3).

As mentioned above, in general a compromise needs to be made between the energy efficiency and the total conversion, since the conversion increases but the energy efficiency drops with higher SEI. Nevertheless, this trade-off is less severe than expected. Increasing the SEI over five orders of magnitude results in almost the same rise in conversion, while the energy efficiency drops only by 44–67% (depending on the gas mixture). This clearly demonstrates that it is not interesting to work at low SEI values to optimize the energy efficiency, since the gain in energy efficiency is negligible compared to the enormous loss in conversion.

In order to be competitive with current technologies and to reduce end-of-pipe gas separation costs, a conversion of 50–80%, comparable with current DRM plants, would be preferred. This is achievable with a DBD, as is clear from Fig. 6, but it requires an SEI in the order of 100 J cm^{-3} , resulting in energy efficiencies of 8.5 to 3.7%, depending on the gas mixture.

Conclusions

In this paper we have studied the influence of the operating parameters (gas mixture, power, residence time and “frequency”) of a dielectric barrier discharge plasma on the

conversion and energy efficiency, to investigate which of these parameters lead to the most promising results and whether these are eventually sufficient for industrial implementation.

The obtained conversion of 84% with an energy efficiency of 8.5% can be considered as the best results in terms of both energy efficiency and conversion. The parameters leading to this result were an SEI of 100 J cm^{-3} , a 10–90 $\text{CH}_4\text{-CO}_2$ ratio, 10 Hz, a residence time of 1 ms. In general we found that increasing the amount of CO_2 in the mixture led to an increase in conversion and energy efficiency. While increasing the SEI, which couples the effect of the power and residence time, only resulted in an increased conversion, but saw a slight decrease in energy efficiency. The most complicated effect was that of the frequency, in the end it was unravelled that it was rather the product of frequency (f) and residence time (τ), *i.e.* the total number of micro-discharge filaments which the gas molecules experience when passing through the reactor, which was critical here. For most cases passing a higher number of filaments (with less energy per filament) yielded higher values for conversion and energy efficiency.

Furthermore, the maximum (theoretical) energy efficiency predicted in this study lies between 11.4 and 15.1%, depending on the $\text{CH}_4\text{-CO}_2$ ratio, which clearly demonstrates that there is still room for improvement for the experiments reported to date, by careful selection of the operating conditions. However, when comparing this maximum theoretical value with the

maximum theoretical energy efficiency obtained for classical thermal DRM, *i.e.*, around 60%, it is clear that when the energy efficiency is the “key performance indicator”, a classical DBD is not competitive. On the other hand, its ease of use (incl. its fast start-up and switch-off, which can save a lot of energy when DRM is combined with other technologies such as fuel cells), its scale-up possibilities as demonstrated for ozone generation and gas cleaning¹⁸ and its capability to convert peak currents from renewable energy sources will probably still give it an advantage over the classical DRM process. Nevertheless, keeping in mind that other alternative techniques can also take advantage of the same peak renewable energy,⁶ it is clearly more interesting from a combined economic and ecologic point of view to focus on other plasma reactor types, for which already higher energy efficiencies have been obtained (see Table 3). This includes microwave discharges,⁸ gliding arcs^{8,13,14} and packed bed DBDs.¹² In the latter case, a DBD is filled with a packing, yielding higher energy efficiencies, *i.e.*, up to a factor 12, as demonstrated already for air pollution control.³⁴ Moreover, this packing can be made of catalytic material, yielding plasma-catalysis.^{7,35} This has the additional advantage that the selectivity towards value-added chemicals and fuels (such as methanol, formaldehyde, formic acid, *etc.*) can greatly be improved, making plasma technology very promising for the dry reforming of methane.

Acknowledgements

The authors acknowledge financial support from the IAP/7 (Inter-university Attraction Pole) program ‘PSI-Physical Chemistry of Plasma-Surface Interactions’, financially supported by the Belgian Federal Office for Science Policy (BELSPO), as well as the Fund for Scientific Research Flanders (FWO). This work was carried out in part using the Turing HPC infrastructure at the CalcUA core facility of the Universiteit Antwerpen, a division of the Flemish Supercomputer Center VSC, funded by the Hercules Foundation, the Flemish Government (department EWI) and the University of Antwerp. Financial support of this work by the UK Engineering and Physical Sciences Research Council (EPSRC) CO2Chem Network and Knowledge Exchange (KE) fund of the University of Liverpool is also gratefully acknowledged.

Notes and references

- 1 Contribution of Working Group I to the Fourth Assessment Report of the Intergovernmental Panel on Climate Change, *Climate Change 2007: The Physical Science Basis*, ed. S. Solomon, D. Qin, M. Manning, M. Marquis, K. Averyt, M. B. Tignor, H. L. Miller and Z. Chen, Cambridge University Press, New York, 2007.
- 2 J. H. Lunsford, *Catal. Today*, 2000, **63**, 165–174.
- 3 A. T. Ashcroft, A. K. Cheetham, M. L. H. Green and P. D. F. Vernon, *Nature*, 1991, **352**, 225–226.
- 4 M. C. J. Bradford and M. A. Vannice, *Catal. Rev.: Sci. Eng.*, 1999, **41**, 1–42.
- 5 J. R. H. Ross, *Catal. Today*, 2005, **100**, 151–158.
- 6 M. Mikkelsen, M. Jørgensen and F. C. Krebs, *Energy Environ. Sci.*, 2010, **3**, 43.
- 7 S. Samukawa, M. Hori, S. Rauf, K. Tachibana, P. Bruggeman, G. Kroesen, J. C. Whitehead, A. B. Murphy, A. F. Gutsol, S. Starikovskaia, U. Kortshagen, J.-P. Boeuf, T. J. Sommerer, M. J. Kushner, U. Czarnetzki and N. Mason, *J. Phys. D: Appl. Phys.*, 2012, **45**, 253001.
- 8 X. Tao, M. Bai, X. Li, H. Long, S. Shang, Y. Yin and X. Dai, *Prog. Energy Combust. Sci.*, 2011, **37**, 113–124.
- 9 R. Snoeckx, R. Aerts, X. Tu and A. Bogaerts, *J. Phys. Chem. C*, 2013, **117**, 4957–4970.
- 10 Z. Jiang, T. Xiao, V. L. Kuznetsov and P. P. Edwards, *Philos. Trans. R. Soc., A*, 2010, **368**, 3343–3364.
- 11 M. E. Dry, *Catal. Today*, 2002, **71**, 227–241.
- 12 Q. Wang, Y. Cheng and Y. Jin, *Catal. Today*, 2009, **148**, 275–282.
- 13 A. Indarto, J. Choi, H. Lee and H. Song, *Energy*, 2006, **31**, 2986–2995.
- 14 X. Tu and J. C. Whitehead, *Int. J. Hydrogen Energy*, 2014, **39**, 9658–9669.
- 15 A. Fridman, *Plasma chemistry*, Cambridge University Press, New York, 2008.
- 16 A. Gutsol, A. Rabinovich and A. Fridman, *J. Phys. D: Appl. Phys.*, 2011, **44**, 274001.
- 17 R. Dorai, K. Hassouni and M. J. Kushner, *J. Appl. Phys.*, 2000, **88**, 6060–6071.
- 18 U. Kogelschatz, *Plasma Chem. Plasma Process.*, 2003, **23**, 1–46.
- 19 R. Snoeckx, M. Setareh, R. Aerts, P. Simon, A. Maghari and A. Bogaerts, *Int. J. Hydrogen Energy*, 2013, **38**, 16098–16120.
- 20 R. Aerts, T. Martens and A. Bogaerts, *J. Phys. Chem. C*, 2012, **116**, 23257–23273.
- 21 R. Aerts, X. Tu, W. Van Gaens, J. C. Whitehead and A. Bogaerts, *Environ. Sci. Technol.*, 2013, **47**, 6478–6485.
- 22 R. Aerts, R. Snoeckx and A. Bogaerts, *Plasma Process. Polym.*, 2014, **11**, 985–992.
- 23 C. Xu and X. Tu, *J. Energy Chem.*, 2013, **22**, 420–425.
- 24 R. Aerts, W. Somers and A. Bogaerts, *ChemSusChem*, 2015, **8**, 702–716.
- 25 Q. Wang, B.-H. Yan, Y. Jin and Y. Cheng, *Plasma Chem. Plasma Process.*, 2009, **29**, 217–228.
- 26 V. Goujard, J.-M. Tatibouët and C. Batiot-Dupeyrat, *Appl. Catal., A*, 2009, **353**, 228–235.
- 27 X. Zhang and M. S. Cha, *J. Phys. D: Appl. Phys.*, 2013, **46**, 415205.
- 28 X. Tu and J. C. Whitehead, *Appl. Catal., B*, 2012, **125**, 439–448.
- 29 J. H. Lozano-Parada and W. B. Zimmerman, *Chem. Eng. Sci.*, 2010, **65**, 4925–4930.
- 30 U. Kogelschatz, *Contrib. Plasma Phys.*, 2007, **47**, 80–88.
- 31 T. Kozák and A. Bogaerts, *Plasma Sources Sci. Technol.*, 2014, **23**, 045004.
- 32 Y. Zhang, Y. Li, Y. Wang, C. Liu and B. Eliasson, *Fuel Process. Technol.*, 2003, **83**, 101–109.
- 33 A. Ozkan, T. Dufour, G. Arnoult, P. De Keyser, A. Bogaerts and F. Reniers, *J. CO2 Util.*, 2015, **9**, 74–81.
- 34 H. L. Chen, H. M. Lee, S. H. Chen and M. B. Chang, *Ind. Eng. Chem. Res.*, 2008, **47**, 2122–2130.
- 35 E. C. Neyts and A. Bogaerts, *J. Phys. D: Appl. Phys.*, 2014, **47**, 224010.